

Kinetic Processes in the Electric Discharge in SF₆

Yu. I. Bychkov, S.A. Yampolskaya, A. G. Yastremskii

*High-Current Electronics Institute, Siberian Division, Russian Academy of Sciences,
Akademicheskii pr. 2/3, Tomsk, 643055 Russia
e-mail: yastrems@lgl.hcei.tsc.ru*

Abstract - The simulation of the kinetic processes in the spatially homogeneous and heterogeneous plasma of the gas discharge in SF₆ is performed. The calculated time dependences of the rates of the most important processes and the concentrations of electrons, ions, and other particles that affect the plasma characteristics are presented. The calculated and experimental results are compared. The kinetic processes are analyzed and their effect on the plasma characteristics is demonstrated. The calculated data regarding the development of the plasma channel are presented. An increase in the conductivity inside the channel is discussed.

1. Introduction

Recent interest in the properties of discharge in gas mixtures based on SF₆ has been driven by the diversified applications of this gas in electronic and switching circuits and in pulsed HF/DF lasers. The dielectric properties of SF₆ are used in high-voltage devices. However, the physics of such an electric discharge is poorly studied and the discharge properties are not fully used. Chemical HF/DF lasers are promising sources of coherent radiation that deliver high-energy radiation in the wavelength range 2.4–3.2 μm. In 1971, lasing on the vibrational transitions of the HF molecule in the discharge-excited C3 H8/He/SF₆ mixture was reported in [1]. We note the recent progress in the development of pulsed HF/DF lasers. Nevertheless, the limiting properties of the gas mixtures used as laser active media remain unknown. The realization of the limiting characteristics will make it possible to reach higher specific parameters and to significantly increase the laser efficiency.

The volume character of the current flow is a necessary condition for effective energy input to the discharge, an increase in the concentrations of particles to the desired level, and effective energy extraction. Discharge contraction impedes the improvement of the discharge spatial homogeneity. This effect lies in the discharge plasma transformation from the state of volume burning to the state with a single or a few plasma channels.

The formation of plasma channels depends on the discharge gap configuration, the composition of the gas mixture, and the parameters of the pump electric circuit.

A comprehensive interpretation of the physical reasons for the channel formation in the SF₆ gas mixtures and the corresponding plasma properties is missing.

The increasing amount of works aimed at the study of the HF lasers accounts for the noticeable results on the increase in laser energy and efficiency. In a series of experimental works supervised by Firsov [2], radiation pulse energy of hundreds of joules is realized in lasers with pumping initiated by electric discharge. An energy of 144 J and an efficiency of 2.8% were obtained on a setup with a discharge region size of 15 x 15 x 75 cm³ in the absence of a preionization source with a mixture consisting of SF₆ and ethane [2]. In the HF (DF) laser with a discharge region size of 27 x 20 x 100 cm³, the radiation energy is 397 (312) J and the efficiency is 3.8% (3%). These characteristics are realized owing to the high spatial homogeneity of the discharge and the large volume of the discharge gap.

Plasma instability is the main problem in the electric discharge pumping of pulsed lasers. The improvement of the pumping schemes and the optimization of the excitation conditions may lead to a further increase in the energy characteristics of HF lasers. Pumping optimization lies in the realization of the needed electric characteristics of plasma while maintaining the plasma spatial homogeneity during the pump pulse. SF₆ is a gas that determines the discharge properties in the SF₆-containing mixtures. The remaining components of the active medium (neon, fluorine, hydrogen, etc.) affect the discharge characteristics much more weakly. Therefore, in this work, the experimental study and the simulation of the kinetic processes are performed for gas discharge in SF₆.

The simulation is carried out for both homogeneous and inhomogeneous discharge plasmas. It yields the time dependences of the rates of the dominating processes and the concentrations of electrons, ions, and other particles that affect the plasma characteristics. The results of the calculations are compared with the experimental data. The kinetic processes are analyzed and the effect of these processes on the plasma characteristics is demonstrated. The calculated evolution of the plasma channel is presented and the conductivity growth in such a channel is discussed.

2. Discharge model

2.1. 0D Model

A self-consistent 0D model is built on the assumption of the local character of the electric field and the spatial homogeneity of the discharge. The model involves (i) the Boltzmann equation for the calculation of the electron energy distribution function (EEDF), (ii) a system of balance equations that describe the time variations in the concentrations of electrons and heavy particles, (iii) an equation for the calculation of gas temperature, and (iv) an equation for the external electric circuit. We solve the quasistationary Boltzmann equation using the method of weighted residuals [3] with allowance for the elastic, inelastic, and electron-electron collisions and collisions of the second kind.

The system of balance equations describes the time variations in the concentrations for more than 40 particles: electrons e^- , negative and positive ions F_2^- , SF_4^- , SF_5^- , SF_6^- , F_4^+ , SF_5^+ , SF_6^+ , F_2^+ and neutral plasma particles.

In general, the kinetic model is similar to the model from [4]. The difference lies in the fact that the model takes into account the stepwise ionization of the SF6 (f) molecule in the excited electronic state [5]. The cross sections of the electron interaction with the components are taken from [6, 7].

We test the model using the experimental data obtained at the High-Current Electronics Institute [8,9] and alternative data from [5]. The tests show that the experimental data are in good agreement with the results of the calculations in a wide range of charging voltages of the capacitor bank and the discharge current densities.

2. 2D Model

The spatial heterogeneities of the discharge are simulated in the framework of a self-consistent 2D model. This model does not take into account the development of the cathode spot and the near-electrode processes. The plasma channel is initiated in the discharge gap in the presence of the initially heterogeneous electric field. A heterogeneity that represents a metal hemisphere with a characteristic size of 0.1 cm is located at the center of the cathode. The main problem of the simulation lies in the search for the processes that most strongly affect the formation of the plasma channel developing from the local heterogeneity on the cathode.

The 2D model employs the condition for the local character of the electric field: at each point of the discharge, the constants of the reactions that involve electrons and the transport coefficients depend on the electric field strength at this point. At each mesh point, we solve the Boltzmann equation with allowance for all the channels in which the electron energy decreases

and the system of the balance equations for the aforementioned particles used in the 0D model.

The electric field strength is derived from the following equation:

$$\operatorname{div}(\mathbf{j}) = e\mu (n_e \operatorname{div}(\mathbf{E}) + \mathbf{E} \operatorname{grad}(n_e)) = 0 \quad (1)$$

We assume that, at each point of the discharge gap with the electron concentration gradient, the electric field induces plasma polarization, so that the equilibrium charge is established [10]:

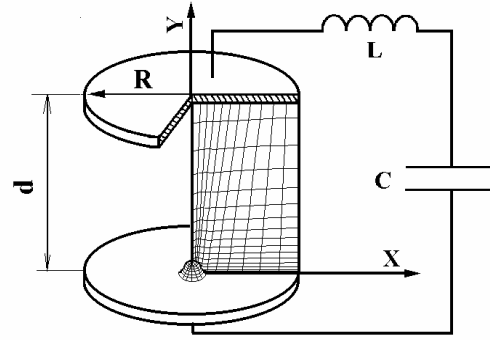


Fig.1 Electrode circuit and an example of the mesh: $d = 2.5$ cm is the interelectrode distance, $R = 1$ cm, $r = 0,1$ cm is the heterogeneity radius, $C = 36$ nF, $L = 9.2$ nH

$$\rho = -\varepsilon_0 \operatorname{div}(\mathbf{E}) = -\varepsilon_0 \frac{\mathbf{E} \operatorname{grad}(n)}{n} \quad (2)$$

Here, \mathbf{j} is the discharge current density, e is the electron charge, μ is the electron mobility, and n is the electron concentration. We assume that the mobilities of electrons and ions are constant. We solve the system of the balance equations and Eq. (1) with the Gear method and the method of weighted residuals [3], respectively, using curvilinear nonorthogonal meshes. Below, we present the results obtained for 60×60 meshes. Figure 1 shows the scheme of the discharge gap and the mesh. Fig. 1 shows the scheme of the discharge gap and the mesh

3. Results and discussion

The calculation results are performed for the initial parameters which corresponds to the experimental results [5]. Fig. 2 demonstrates temporal evolutions of discharge voltage and discharge currents calculated using 0D and 2D models. The discharge voltage is about 20 kV at a maximum discharge current of 8 kA. When the discharge is extinguished, the residual capacitor voltage is about 14 kV. The peak current and residual voltage are in a good agreement with experi-

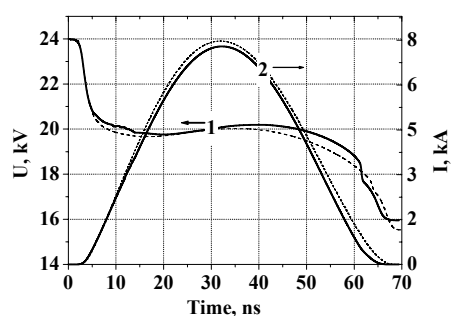


Fig.2 Temporal evolutions of the discharge voltage - 1, and discharge current - 2. Solid lines – are the 0D model results, dashed lines - are the 2D model results

mental results [5]. The difference between the peak current predicted by 2D model and one predicted by 0D model is negligible.

Our simulation shows that plasma channel is formed in the discharge at $t=10$ ns. Fig. 3 A,B demonstrates the spatial distributions of electron density and vibrationally excited molecules of $SF_6(v)$ at this time moment. The concentration of $SF_6(v)$ molecules and electron density in the axis of plasma channel is more than in the homogeneous region. The maximum electrons density observed on top of heterogeneity is $n_e = 1.2 \cdot 10^{15} \text{ cm}^{-3}$. In the region of anode the electron density ($n_e = 2.5 \cdot 10^{14} \text{ cm}^{-3}$) is higher by order of magnitude than the electron density ($n_e = 2.0 \cdot 10^{13} \text{ cm}^{-3}$) in the region of homogeneous discharge.

The same picture we can see for the spatially distribution of the vibrationally excited $SF_6(v)$ molecules. The maximum $SF_6(v)$ concentration observed on the top of heterogeneity ($n = 9.0 \cdot 10^{16} \text{ cm}^{-3}$) decreases in the region of the anode ($n = 9.0 \cdot 10^{16} \text{ cm}^{-3}$). It follows from the calculation results that these molecules play the important role in the kinetics processes. The rate of electron attachment to the $SF_6(v)$ molecules is sig-

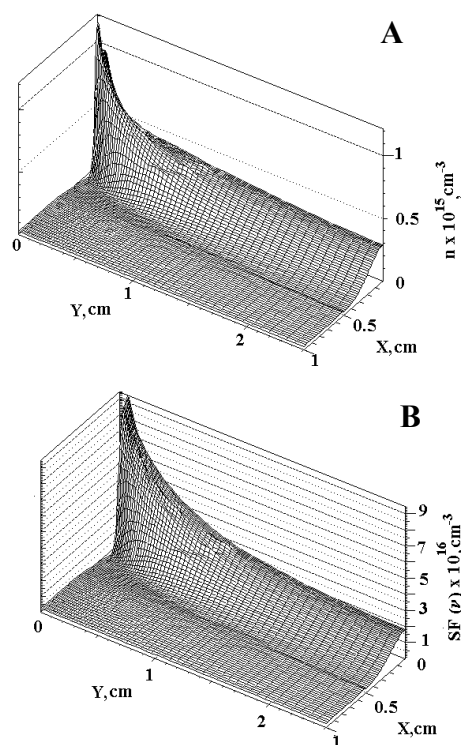


Fig.3 Spatial distribution of electron concentration – A and $SF_6(v)$ concentration - B at $t = 10$ ns

nificant higher than the rate attachment to the $SF_6(0)$ molecules. Therefore the increasing of concentration of vibrationally excited $SF_6(v)$ molecules in the axis of plasma channel lead to increasing of electron attachment frequency in this region. The spatial structure of the discharge become unstable. The plasma channel, formed at first 10 ns of the discharge, disappear. Then the plasma channel is formed again. The similar behaviour of the discharge was observed experimentally in [11].

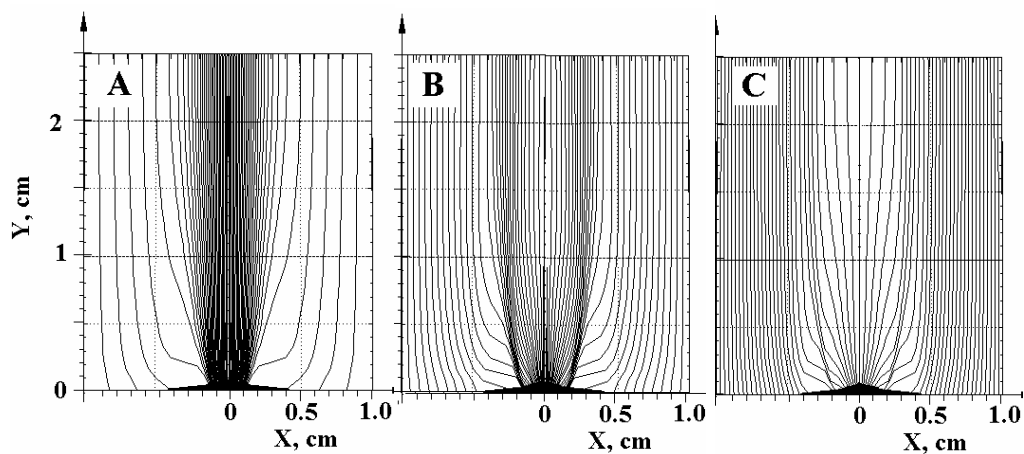


Fig. 4 Current lines at time $t = 10$ ns (A), $t = 16$ ns (B) and $t = 22$ ns (C)

Fig.4 shows a current distribution in the cross section of the plasma channel. This value of current between any two neighboring current lines is 1/60 part of current, flows in layer of unit thickness. It can be seen that the plasma channel arises at the formation stage of the discharge ($t = 10$ ns) and then disappears. The temporal evolution of the electron density and the concentration of vibrationally excited $SF_6(v)$ molecules in every points is the course of such behavior of the discharge. Fig. 5 shows the temporal evolutions of the electron density, concentration of vibrationally excited $SF_6(v)$ molecules, SF_6^* in electronically excited levels, and positively charged ions SF_5^+ near the cathode. The electron density peak ($n_e = 1.2 \cdot 10^{15} \text{ cm}^{-3}$) observed at $t = 10$ ns, disappears at $t = 22$ ns. But concentration of $SF_6(v)$ continue increases up to $t = 20$ ns, causing increasing of attachment frequency of electrons to $SF_6(v)$ molecules. Decreasing of $SF_6(v)$ concentration in the space of further $\Delta t = 10$ ns causes decreasing of attachment frequency and it leads to

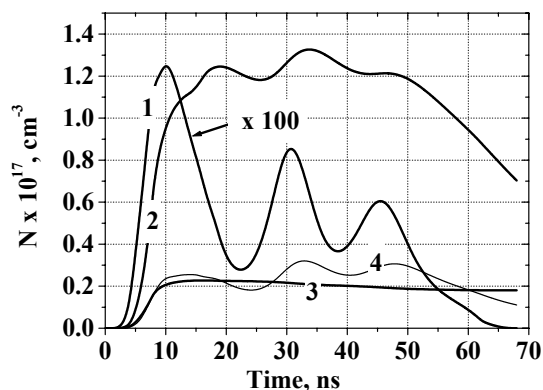


Fig. 5 Temporal evolutions of electron density- 1, concentration of $SF_6(v)$ - 2, SF_6^* - 3, and SF_5^+ - 4 on top of the heterogeneity.

further increasing of electron density. The similar dynamic of electron density and concentration of $SF_6(v)$ molecules takes place in every point of plasma channel axis. In the region of anode electron density achieves the maximum value ($n_e = 3.0 \cdot 10^{14} \text{ cm}^{-3}$) at the same time ($t = 10$ ns), and then one decrease to value less then the electron density in region of homogeneous discharge.

The results of the calculation illustrate the dynamics of the spatial structure of discharge in SF_6 . The plasma channel, formed at the stage of discharge formation, is disappeared at the end of the current pulse.

References

- [1]. T. J. Jacobson, and J. H. Kimpbell, *J. Appl. Phys.* **42** (9), 3402 (1971).
- [2]. V. V. Apollonov, S. Yu. Kazantsev, V. F. Oreshkin, and K. N. Firsov, *Kvantovaya Elektron. (Moscow)* **25** (2), 124 (1998)
- [3]. C. A. J. Fletcher, *Computational Galerkin Methods* (Springer-Verlag, New York, 1984; Mir, Moscow, 1988).
- [4]. L. Richeboeuf, S. Pasquiers, M. Legentil, and V. Puech, *J. Phys. D: Appl. Phys.* **31**, 373 (1998).
- [5]. Yu. Bychkov, S. Gortchakov, B. Lacour, *et al.*, *J. Phys. D: Appl. Phys.* **36**, 380 (2003).
- [6]. V. Puech (private communication).
- [7]. L. G. Christophorou and J. Olthoff, *J. Phys. Chem. Ref. Data* **29** (3), 267 (2000).
- [8]. Yu. I. Byskov, S. L. Gorchakov, and A. G. Yastremskii, *Izv. Vyssh. Uchebn. Zaved. Fiz.* **8**, 43 (1999).
- [9]. Yu. Bychkov, S. Gortchakov, and A. Yastremskii, *Quantum Electron.* **30**, 733 (2000).
- [10]. Yu. Bychkov, S. Gortchakov, S. Yampolskaya, and A. Yastremskii, *Proc. SPIE* **4047**, 106 (2002).
- [11]. V. V. Apollonov, A. A. Belevtsev, S. Yu. Kazantsev, *et al.*, *Kvantovaya Elektron. (Moscow)* **32** (2), 92 (2003)